

Coulomb interaction effects and electron spin relaxation in the one-dimensional Kondo lattice model

Sebastian Smerat*

Physics Department, Arnold Sommerfeld Center for Theoretical Physics, Ludwig-Maximilians-Universität München, D-80333 München, Germany

Herbert Schoeller

Institut für Theorie der Statistischen Physik and JARA-Fundamentals of Future Information Technology, RWTH Aachen University, D-52056 Aachen, Germany

Ian P. McCulloch

School of Physical Sciences, University of Queensland, Queensland 4072, Australia

Ulrich Schollwöck

Physics Department, Arnold Sommerfeld Center for Theoretical Physics and Center for NanoScience, Ludwig-Maximilians-Universität München, D-80333 München, Germany

(Received 15 November 2010; revised manuscript received 11 January 2011; published 25 February 2011)

We study the effects of the Coulomb interaction in the one-dimensional Kondo lattice model on the phase diagram, the static magnetic susceptibility, and electron spin relaxation. We show that onsite Coulomb interaction supports ferromagnetic order and nearest-neighbor Coulomb interaction drives, depending on the electron filling, either a paramagnetic or a ferromagnetic order. Furthermore, we calculate electron quasiparticle lifetimes, which can be related to electron spin relaxation and decoherence times, and explain their dependence on the strength of interactions and the electron filling in order to find the sweet spot of parameters where the relaxation time is maximized. We find that effective exchange processes between the electrons dominate the spin relaxation and decoherence rate.

DOI: [10.1103/PhysRevB.83.085111](https://doi.org/10.1103/PhysRevB.83.085111)

PACS number(s): 71.10.Li, 71.27.+a, 73.21.Hb

I. INTRODUCTION

Recently, the interest in nanoscale systems has been rapidly increasing. Among them are ^{13}C carbon nanotubes,^{1,2} nanowires,^{3,4} and carbon nanotubes filled with endohedral fullerenes or molecular magnets.⁵ The above-mentioned systems have in common that they consist of local spins (electron or nuclear spins) which interact via exchange interaction with itinerant conduction electrons. These are exactly the constituents of the one-dimensional Kondo lattice model^{6,7} (KLM). To make these materials available for spin electronics or quantum information processing, it is necessary to understand their properties in detail: ground-state (e.g., magnetic order), spectral (e.g., dispersion relation of electrons), and dynamical (e.g., nonequilibrium, spin relaxation/decoherence) properties.

Interaction between the local spins in the KLM is generated effectively due to the hopping t of electrons and an onsite direct spin exchange J between the itinerant and localized spins (see Fig. 1). This interaction is a result of the competition of onsite singlet formation and an effective Ruderman-Kittel-Kasuya-Yosida (RKKY) interaction.⁸ The order of the local spins due to the interaction is captured in the phase diagram of the KLM,^{6,9–12} which is basically divided into three phases depending on J/t and the electron filling n ($n = 1$ is half filling). At $n = 1$ the system turns out to order antiferromagnetically for arbitrary coupling strength. A ferromagnetic (FM) phase is established, if either J is large enough or n is small enough.¹³ Otherwise, the local spin lattice is in the paramagnetic (PM) phase, because then the effective RKKY interaction dominates the system.

The mechanism of ferromagnetism in the KLM can also be understood in terms of an electron quasiparticle picture, where the quasiparticle is the so-called *spinpolaron*^{14,15} [see Fig. 2(a)]. For a given FM order of the local spins in an one-dimensional (1D) system it was shown that the itinerant electrons and the magnons of the local spin bath form a bound spinpolaron state which is detectable in transport measurements and was proposed as a long-living correlated many-body spin state³ forming possibly one part of a many-body spin qubit. In Ref. 13 it was shown for the case of a single conduction electron that a spinpolaron develops with a huge extent over the whole lattice leading to FM order in the ground state. In Ref. 16 this was extended to finite electron fillings and it was shown that long quasiparticle lifetimes are connected with FM order of the local spins. In Ref. 17, the quasiparticle dynamics of the half-filled KLM ($n = 1$) have been examined as well. By means of a strong coupling expansion up to 11th order it has been possible to calculate the quasiparticle dispersion relation to good accuracy and it could be shown that the quasiparticles behave like nearly localized f electrons due to the strong correlation of the conduction and localized electrons.

It is known that the main relaxation and decoherence source of single electron spins in semiconductor-based quantum dots arises from interactions with the nuclear spin background.^{18–20} An appropriate path to diminish the relaxation is the application of a large magnetic field, whereas the decoherence rate is reduced by state distribution narrowing.^{21,22} However, the initial preparation of the nuclear bath in a pure state (e.g., full polarization) is an experimental challenge. Recently,

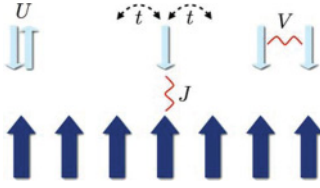


FIG. 1. (Color online) The KLM. The conduction electrons are depicted in the upper row (light blue) and the localized electrons are depicted as bold arrows in the lower row (dark blue).

the idea was proposed to consider the nuclear bath at very low temperatures in the FM phase, which is mediated by many itinerant electrons via the RKKY interaction.^{2,3,16,23} In Ref. 2 it was shown that the Coulomb interaction in a 2D electron gas leads to an increased critical temperature of order $T \sim 1$ mK for the nuclear spins, which might be feasible in experiments. In Ref. 23 a ¹³C carbon nanotube was studied. By approximating the conduction electrons by a Luttinger liquid and treating the large effective nuclear spins classically, the transition temperature between a helically ordered (FM for finite systems) and unordered spin lattice was calculated.²³ It could be shown that a finite long-ranged Coulomb interaction is required to have a finite transition temperature,² which is consistent with the Mermin-Wagner theorem²⁴ and its recent extension.²⁵ Taking backaction effects of the nuclear lattice on the electron spins into account increases the transition temperature by another order of magnitude. This makes the KLM interesting for experiments, which are always performed at finite temperature.

These developments motivate the study of the KLM in the presence of a finite Coulomb interaction between the itinerant electrons. The simplest extension to the KLM in terms of lattice models is the onsite Coulomb interaction U . In the case of half filling a finite U leads to the opening of a spin and charge gap.²⁶ This work has been extended within a continuum Luttinger liquid approach to arbitrary fillings solved by bosonization.²⁷ Lattice effects have been accounted for by means of a phononic field and therefore there is no real lattice involved in those calculations. Still, the authors of Ref. 27 find the interesting result of a shift of the phase boundary between FM and PM phase, as expected.

In this paper, we use the density matrix renormalization group (DMRG) method^{28–31} to study ground-state and dynamical properties of the 1D KLM for local spins with spin-1/2 including onsite and nearest-neighbor Coulomb interaction. Our method benefits from being numerically exact, acting in the lattice space without any approximations, and taking all backaction effects of the local spin lattice on the conduction electrons automatically into account. Furthermore, it allows for

calculations in a broad parameter regime and works especially well for 1D systems with open boundary conditions and finite lattices. Here, we are particularly interested in finite lattices, since nanoscale systems have finite sizes and show corresponding effects. Considering other but open boundary conditions, for example, periodic boundary conditions, leads to methodical difficulties of the DMRG method. The influence of the boundaries on the lifetime remains uncertain. However, the experimental situation is described best by open boundaries.

From ground-state calculations we show that onsite Coulomb interaction lowers the value of J required for a transition from a PM to a FM ground state. For small $n \lesssim 0.4$ nearest-neighbor Coulomb interaction V acts the same way on the magnetic order as U does. For $n \gtrsim 0.4$ they compete with each other. As a different sensor of magnetic order we utilize the static electron spin susceptibility. For the PM phase a peak at $2k_F$ is expected (which diverges for $L \rightarrow \infty$), while for the FM order a minimum at the smallest possible quasimomentum q , which is finite for finite lattices, should emerge. This was stated similarly in Refs. 2 and 23 for small coupling constants J .

Finally, we calculate the quasiparticle lifetime broadening Γ_+ of an electron, its spin oriented in the opposite direction than that of all other electrons in the ground state. In Ref. 16 it was shown in the FM phase and for electronic densities below half-filling that the effective interaction between spinpolaron states is weak proving that spinpolaron (spin-down) states are indeed well-defined quasiparticles with small lifetime broadening Γ_- even in the presence of many electrons. However, we show here that the spin relaxation and decoherence rates will be dominated by the lifetime broadening Γ_+ of the opposite spin-up state, which is higher in energy. We consider a single spin-up electron with quasimomentum k on top of the FM ground state of the 1D KLM. Although this spin has the same direction as the underlying local spins and, thus, cannot decay by direct exchange with the local spins, we find that Γ_+ is dominated by the effective exchange interaction with the sea of spinpolaron spin-down states in the system. As a consequence, Γ_+ turns out to be much larger than Γ_- and dominates the spin relaxation as well as the spin decoherence rate (the pure dephasing term arising from the lifetime broadening Γ_- of the spin-down spinpolaron state is negligible). We analyze the lifetime broadening Γ_+ depending on J , U , n , and the quasimomentum k and give explanations for the observations. Although the spin relaxation rate increases significantly in the presence of many electrons we show in appropriate parameter regimes that the spin relaxation rate can be several orders of magnitude smaller in the FM phase compared to the PM phase.

II. MODEL

The Hamiltonian of the KLM with Coulomb interaction is sketched in Fig. 1 and defined as

$$H = -t \sum_{\sigma,i=1}^{L-1} (c_{i\sigma}^\dagger c_{i+1\sigma} + c_{i+1\sigma}^\dagger c_{i\sigma}) + J \sum_{i=1}^L \mathbf{S}_i \cdot \mathbf{s}_i + U \sum_{i=1}^L n_{i\uparrow} n_{i\downarrow} + V \sum_{i=1}^{L-1} n_i n_{i+1}, \quad (1)$$

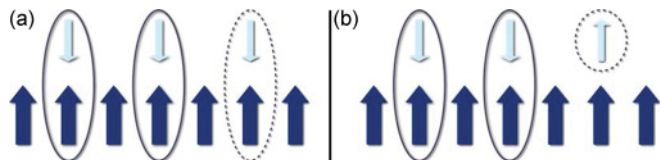


FIG. 2. (Color online) (a) Sketch of a configuration with three spinpolarons, each consisting of a delocalized spin singlet state with the local spins. (b) Sketch of a configuration with two spinpolarons and one spin-up electron.

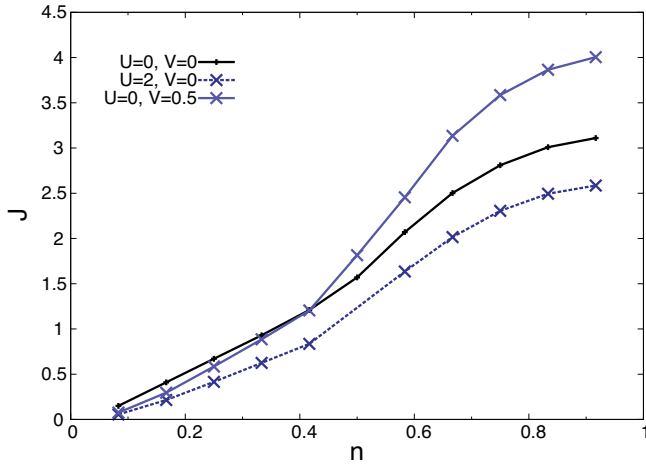


FIG. 3. (Color online) Phase boundary between the FM (upper part) and the PM (lower part) ground state of the KLM with $L = 48$ for three different cases of Coulomb interaction.

where t is the hopping integral, L the lattice size, $c_{i\sigma}^{(\dagger)}$ the electron annihilation (creation) operator at site i with spin σ , $J > 0$ the antiferromagnetic Kondo exchange coupling, S_i the spin operator of the local spin at site i , s_i the spin operator of the conduction electron at site i , U the onsite Coulomb interaction constant, $n_{i\sigma} = c_{i\sigma}^\dagger c_{i\sigma}$, V the nearest-neighbor Coulomb interaction constant, and $n_i = n_{i\uparrow} + n_{i\downarrow}$. All spins are considered to be spin 1/2. We define the filling by $n = N/L$, where N denotes the total number of itinerant electrons ($n = 1$ corresponds to half filling).

III. METHOD

A. DMRG

The DMRG method is a well-established numerically exact method for the calculation of ground states, dynamical properties, and time evolution of 1D lattice systems. Our algorithm is formulated in a matrix-product language³² and makes use of Abelian, for example, particle number conservation [U(1)] and non-Abelian, for example, total spin conservation [SU(2)], symmetries. Depending on the symmetry sector, the use of SU(2) symmetries in addition to U(1) symmetries allows for computations up to ten times faster.

B. Ground states

Calculating the ground state of a given system is synonymous to finding the symmetry sector with its corresponding quantum numbers, where the energy is minimal. The ground-state phase diagram of the KLM is shown in Fig. 3 in dependence of the Kondo constant J and the filling n . Fixing J and n leaves the total spin quantum number S as the only free parameter, which distinguishes the order of the ground state; that is, $S = (L - N)/2$ complies with FM order of local spins and $S = 0$ with PM order. We choose SU(2) symmetry for the spin here, first for computational reasons and second because it has the benefit that the states with different total spin quantum numbers are nondegenerate in this case, whereas in U(1) symmetry a partial degeneracy in the total spin in

the direction of quantization exists. Considering Coulomb interaction in addition, we have another two variables that have to be fixed in advance and this means we have a quadruple of variables $\{n, J, U, V\}$, or a 4D phase diagram.

C. Susceptibility

We calculate the static electron spin susceptibility $\chi(\omega = 0)$ by means of Green's functions and the application of dynamical DMRG^{33,34} with generalized minimal residual (GMRES).^{35,36} Details of our implementation can be found in Ref. 16.

The definition of the spin susceptibility is

$$\chi_q^{+-}(\omega) = -\frac{1}{L} \left[\langle 0 | \tilde{s}_q^+ \frac{1}{H - E_0 + \omega - i\eta} \tilde{s}_q^- | 0 \rangle + \langle 0 | \tilde{s}_q^- \frac{1}{H - E_0 - \omega + i\eta} \tilde{s}_q^+ | 0 \rangle \right], \quad (2)$$

with (for open boundary conditions)

$$\tilde{s}_q = \sum_{l=1}^L s_l \sin\left(\frac{ql\pi}{L+1}\right),$$

where H is the Hamiltonian given in Eq. (1), $|0\rangle$ is the ground state of the system, and E_0 the ground-state energy. η is a finite artificial broadening factor, needed to avoid finite size effects³⁰ and which can be chosen smaller with larger lattice size.

D. Quasiparticle lifetimes

In Ref. 16 the quasiparticle lifetime of the spinpolaron was calculated [cf. Fig. 2(a)] by evaluating the electronic Green's function in momentum and frequency space,

$$G_{k\sigma}(\omega + i\eta) = \frac{1}{\omega + i\eta - [\epsilon_0(k) - \mu + \Sigma_\sigma(k, \omega + i\eta)]}, \quad (3)$$

where ω is the energy, $\epsilon_0(k)$ the free electron dispersion relation, μ the electrochemical potential (which does not play a role in the calculation of broadenings of spectral densities), and $\Sigma_\sigma(k, \omega + i\eta)$ the complex self-energy. From the imaginary part of the self-energy, which is given by the broadening of the Lorentzian shaped peak in the spectral density $A_\sigma(k, \omega) = -(1/\pi) \text{Im} G_{k\sigma}(\omega)$ we can determine the quasiparticle lifetime in dependence of all parameters. On the technical side, we use again the above-mentioned GMRES method and calculate spectral densities as described in Ref. 16.

Basically, there exist four different scenarios for which the electronic quasiparticle life-time broadenings can be calculated assuming that in the FM ground state the local spins point up and the conduction electron spins point down (for large J the most dominant part of a spinpolaron state consists of a conduction electron pointing down with a small admixture of the spin-up state plus a local magnon):

- (1) In the FM phase for a spin-down electron [cf. Fig. 2(a)];
- (2) In the FM phase for a spin-up electron [cf. Fig. 2(b)];
- (3) and (4) are the corresponding cases for the PM phase.

Scenario (1) corresponds to the spinpolaron lifetime broadening Γ_- and scenario (2) to its natural counterpart Γ_+ .

Scenarios (3) and (4) are identical, since the spins in the PM ground state have no specific direction.

In addition to Ref. 16 we calculate here the lifetime broadening Γ_+ . As shown in this paper this rate is very large in the presence of many electrons, $\Gamma_+ \gg \Gamma_-$, and, as a consequence, dominates the spin relaxation and decoherence rates, as can be understood from the following qualitative analysis. The two many-body spin states $|\pm\rangle$ depicted in Fig. 2 are not exact eigenstates but are expected to be part of a sharp many-body continuum with long lifetimes. The spin-down state $|-\rangle$ is protected from magnon absorption and emission processes since the spinpolarons can lower their energy by the entanglement with the local spins in a singlet state. Only virtual processes and weak spinpolaron-spinpolaron interactions lead to a small broadening Γ_- of this state, as shown in detail in Ref. 16. The spin-up state $|+\rangle$ is protected due to the spin polarization of the local spins. Due to effective exchange interaction between the spinpolarons and the spin-up electron mediated by the magnons, as discussed in detail in this paper in Sec. IV C, this state has a lifetime broadening $\Gamma_+ \gg \Gamma_-$. Denoting the quasienergies of the two spin states by E_{\pm} , we get a decay according to $\langle \pm | e^{-iHt} | \pm \rangle \sim e^{-iE_{\pm}t} e^{-(\Gamma_{\pm}/2)t}$. To define the spin relaxation and decoherence rates, we introduce pseudospin operators $P_z = (1/2)(|+\rangle\langle +| - |-\rangle\langle -|)$ and $P_{\pm} = |\pm\rangle\langle \mp|$. Using spin conservation, we obtain after a straightforward calculation that $\langle P_z(t) \rangle = (1/2)\langle |+\rangle\langle +| e^{-iHt} |+\rangle|^2$, if the system is prepared at $t = 0$ in the state $|+\rangle$, and $\langle P_+(t) \rangle = (1/2)\langle |+\rangle\langle +| e^{-iHt} |+\rangle^* \langle -| e^{-iHt} |-\rangle$, if the system is prepared in the state $(1/\sqrt{2})(|-\rangle + |+\rangle)$ initially. As a result we find for the two different initial preparations that $\langle P_z(t) \rangle \sim e^{-\Gamma_+ t}$ and $\langle P_+(t) \rangle \sim e^{i\Delta t} e^{-\Gamma_+ t}$, where $\Delta = E_+ - E_-$ is the quasienergy splitting and the spin relaxation/decoherence rates are given by

$$\Gamma_1 = \Gamma_+, \quad \Gamma_2 = \frac{1}{2}\Gamma_+ + \frac{1}{2}\Gamma_- \quad (4)$$

This result shows that the dominant part to $\Gamma_{1/2}$ is given by the broadening Γ_+ of the spin-up state $|+\rangle$, whereas the broadening Γ_- of the spinpolaron state $|-\rangle$ enters only into the pure dephasing term of longitudinal fluctuations and can be neglected.

E. Dispersion relation

The dispersion relation $\omega_{\sigma}(k)$ can be constructed from the resonance of the single-particle spectral density $A_{\sigma}(k, \omega)$ at $\omega = \omega_{\sigma}(k)$. The number of k values is restricted by the lattice size L .

IV. RESULTS

In nearly all cases we have chosen $L = 48$, which is suitable from two different points of view. First, physically, we are especially interested in finite systems, which would more closely resemble, for example, nanotubes in the real world. Second, from the point of view of computational cost, it is not convenient to take larger systems into account, since we already needed up to 3000 DMRG states in some of the calculations, which is a large number considering the number of executed calculations. All calculations are done with high computational precision, partly up to machine precision. We

set $t = 1$ in all calculations, which is therefore the relevant energy unit in all calculations.

A. Phase diagram

We first investigate the influence of Coulomb interaction on the ground state of the KLM. The phase diagram⁶ of the KLM (without Coulomb interaction) is well established and shows two different phases, an FM and a PM one (see Fig. 3). The PM phase lies in the lower-right triangular of the phase diagram and for all other values of J and $n < 1$ the KLM has an FM ground state. Especially for $N = 1$ it was shown that the KLM is FM for any J .¹³ As can be seen from Fig. 3, applying a finite onsite Coulomb interaction shifts the phase boundary downward for all values of n . This is consistent with the analysis of Ref. 23, where a higher crossover temperature has been predicted in the presence of Coulomb interaction. However, we note that the two mechanisms are quite different. Whereas in Ref. 23 the local nuclear spins have been treated quasiclassically due to their large effective spin, the present analysis is in the full quantum-mechanical regime of local spins with spin-1/2. Roughly speaking the present result is consistent with the Stoner picture of ferromagnetism, where a finite Coulomb interaction leads to the preference of a fully spin-polarized state for the itinerant electrons. This state coincides with the qualitative picture of spinpolaron states pointing into the opposite direction of the local spins [see Fig. 2(a)].

For finite nearest-neighbor Coulomb interaction V we find the qualitatively different result that the phase boundary is shifted downward for $n \lesssim 0.4$ and upward for $n \gtrsim 0.4$ and therefore crosses the phase boundary of the KLM without Coulomb interaction. For small fillings this can be explained in the same way as for the onsite Coulomb interaction case. For filling $n > 0.4$ the electrons are relatively close to each other and therefore strongly influenced by V . The possibility to occupy the same site with two electrons of opposite spin does not lead to an increasing energy due to Coulomb interaction and increases the kinetic energy at the same time. Therefore, in this regime, the unordered state becomes more favorable.

Summarizing, the onsite and nearest-neighbor Coulomb interaction are concurring for small $n < 0.4$ and behave competitively for large $n > 0.4$. These results are pictured in Fig. 3: The solid black line is the phase boundary of the noninteracting KLM. If Coulomb interaction is switched on, the phase boundary is lowered for all values of n (dashed dark blue line). For $U = 0$ and V finite, the phase boundary is lowered for small n and raised above the noninteracting case phase boundary for larger n .

B. Susceptibilities

For small J the order of the local spins manifests itself also in the static electron spin susceptibility. As was shown in Ref. 23 the effective coupling between the local spins for small J is

$$J_{\text{RKKY}} \propto -\chi^{\pm}(\omega = 0, k, J, U). \quad (5)$$

Therefore, the order of the local spin lattice should correspond to the absolute maximum of the static electron spin

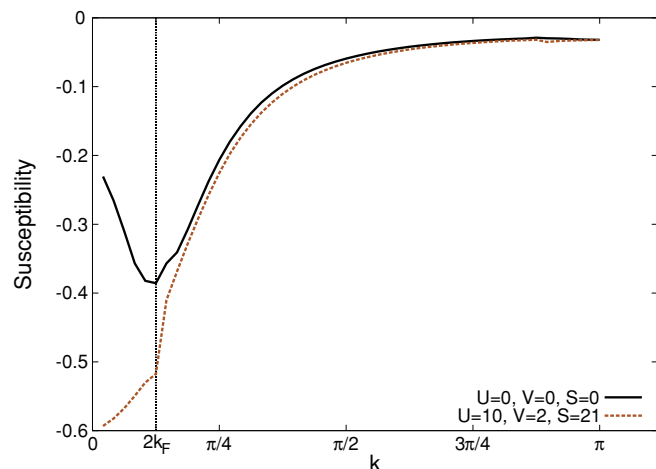


FIG. 4. (Color online) Static electron spin susceptibility $\chi(\omega = 0)$ for a KLM with $L = 48$, $N = 6$, and $J = 0.15$ with (dashed line) and without (solid line) Coulomb interaction. The thin vertical line marks $2k_F$ in the PM phase.

susceptibility. In Fig. 4 we show this for two extreme cases with $L = 48$ and $N = 6$. The first case (solid black line in the figure) with $U = 0$, $V = 0$ has a PM ground state and shows the susceptibility in the noninteracting case. It has an absolute maximum at $k = 2k_F$. This evidences that for the chosen set of parameters the state indeed orders paramagnetically in a RKKY-like fashion. If Coulomb interaction is switched on with $U = 10$, $V = 2$ (dashed brown line in the figure), the absolute maximum is at $k = 0$. In this case FM order becomes dominant.

C. Dispersion relation

We calculated the dispersion relation of a \uparrow electron in a KLM with $L = 48$, $N = 4$, $J = 0.5$, and $U = V = 0$. The result is shown in Fig. 5. It shows a cosine-shaped dispersion, which leads to the conclusion that the electron behaves more or less like a free electron, only slightly affected by the presence of the local spin lattice. This can be explained by the fact that a \uparrow electron cannot flip its spin directly by an exchange process with a local spin due to spin conservation. In contrast, a \downarrow electron can do so, leading to the formation of spinpolarons, which can lower their energy by this process and obtain a larger effective mass leading to a sharper dispersion relation. However, as shown in the next section, the lifetime broadening of \uparrow electrons is generically larger than those of \downarrow electrons, since the decay processes for spinpolarons start in higher order in J than those for \uparrow electrons.

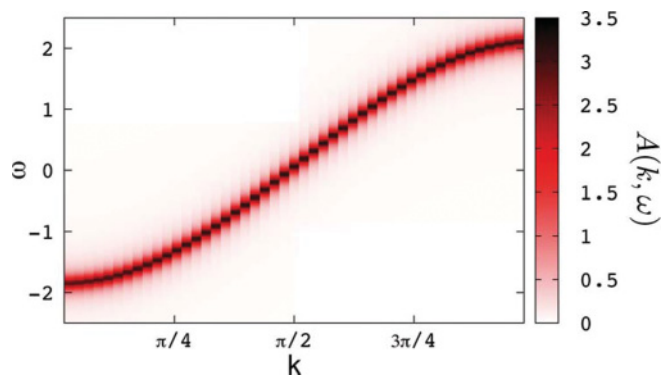


FIG. 5. (Color online) Dispersion relation of a \uparrow electron in a KLM with $J = 0.5$, $N = 4$, and $U = V = 0$.

D. Quasiparticle lifetimes

From the electronic spectral density $A_{\uparrow}(k, \omega)$ we obtain the quasiparticle lifetime broadenings Γ_+ in dependence of J , U , k , and N . As we calculate the Green's function $G_{\uparrow}(k, \omega)$ in frequency space, we obtain two branches: The $c_{k\uparrow}^{\dagger}$ and the $c_{k\uparrow}$ branch, respectively. The first one corresponds to an additional electron placed in a certain k mode and interacting with the other electrons and the local spins. The second type addresses the spin-up part of the already existing electrons in the system. Therefore, the two branches address two different sets of states in the spectrum of the Hamiltonian. Here we are interested in the first case only, since we would like to know what happens to a spin-up electron brought into the system in addition to the other electrons.

1. Decay rate dependence on k

In Table I we show decay rates of a spin-up electron added to the $N = 2$ ground state. For all sets of U and J we find that the decay rate increases with increasing k as long as k is smaller than $2k_F$. Here we give an explanation considering momentum conservation and phase-space arguments. In the FM ground state the lowest electronic orbitals in k space are occupied up to $2k_F$ by the available electrons all with spin-down. A state with wave vector k has quasimomentum $\pm k$ due to the open boundary conditions. An additionally superimposed spin-up electron with a certain wave vector k_1 has to change to the state $k_2 > 2k_F$ in order to flip its spin [see Fig. 7(a)]. This decay channel can only happen if a magnon is absorbed with wave vector $q = |k_1 \pm k_2|$. Such magnons are present in the ground state because each spinpolaron state consisting of a spin-down electron with wave vector k has a small admixture of spin-up states with wave vector $|k \pm q|$ and a local magnon in state q . Smaller values of k_1 decreases the number of magnons with small wave vector $q = |k_1 - k_2|$ to enable this process.

TABLE I. k -dependence of relaxation rates for $N = 2$ for different values of J and U .

$k [\pi/(L+1)]$	1	2	3	4
$J = 0.5, U = 0$	0.00097 ± 0.00003	0.00128 ± 0.00002	0.00166 ± 0.00003	0.00204 ± 0.00005
$J = 0.5, U = 0.2$	0.00220 ± 0.00009	0.00299 ± 0.00005	0.00403 ± 0.00005	0.0048 ± 0.0001
$J = 0.3, U = 0$	0.00035 ± 0.00001	0.000470 ± 0.000004	0.00066 ± 0.00002	0.00077 ± 0.00002
$J = 0.3, U = 0.2$	0.00146 ± 0.00006	0.00198 ± 0.00004	0.00280 ± 0.00007	0.00331 ± 0.00008

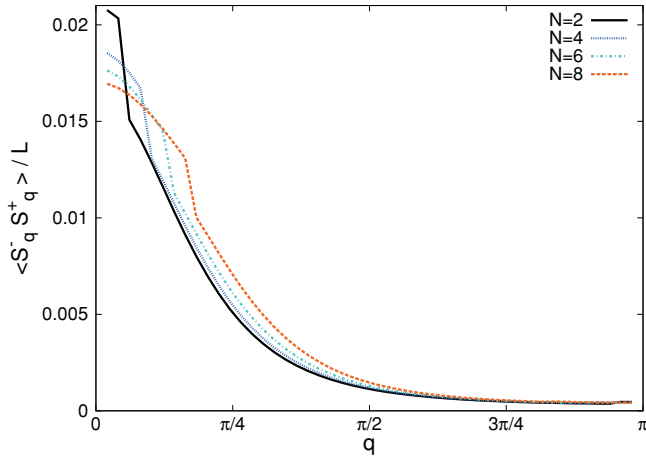


FIG. 6. (Color online) Magnon density in the KLM with $L = 48$, $t = J = 1$, $U = V = 0$ in dependence of the quasimomentum. The number of electrons is varied between two and eight in steps of two.

This can be quantified by the magnon density per electron $m_q = \langle S_q^- S_q^+ \rangle / N$ (see Fig. 6) and further by the accumulated magnon density

$$\rho_{k_1} = \sum_{\sigma=\pm} \sum_{\substack{q = |k_1 + \sigma k_2| \\ 0 < q < \pi, 2k_F < k_2 < \pi}} m_q, \quad (6)$$

which is shown in Fig. 7(b) and clearly states that the number of suitable magnons increases with increasing k_1 even above $2k_F$ until it falls off finally. This result qualitatively reflects the decay rate for the spin-up electron shown in Fig. 7(c) for a KLM with $L = 48$, $N = 4$, $J = 0.5$, and $U = V = 0$. The decay rate first increases for small k as indicated by the accumulated magnon density. For values above $2k_F$ the decay rate even surpasses the values at $2k_F$ until it decreases finally for larger values of k . We note that this is only a qualitative explanation since other decay channels involving absorption of many magnons are present as well.

The discussed process for the decay of the spin-up electron is essentially an exchange process between a spin-up electron in state k_1 and a spinpolaron in state k . The spinpolaron provides the magnon with wave vector $q = |k_1 \pm k_2|$ to flip the spin-up electron from state k_1 to state k_2 , leaving the spinpolaron as a spin-up electron in state $|k \pm q|$. As a result, by mediation of a local magnon, the spins of two electrons have been exchanged, whereas the local spin lattice is unaffected. This spin exchange process is the essential process leading to a large lifetime broadening of the spin-up electrons if many electrons are present in the system. In contrast, the spinpolaron states have lifetime broadenings, which are several orders of magnitude smaller compared to those of the spin-up states. The reason is that the spinpolaron-spinpolaron interaction is rather weak and can only be mediated via multimagnon processes.

2. Decay rate dependencies on U, J, N

In this section we explain how the quasiparticle decay rate of the spin-up state depends on U, J , and N and why the found tendencies are to be expected. The results for these cases are shown in Table II.

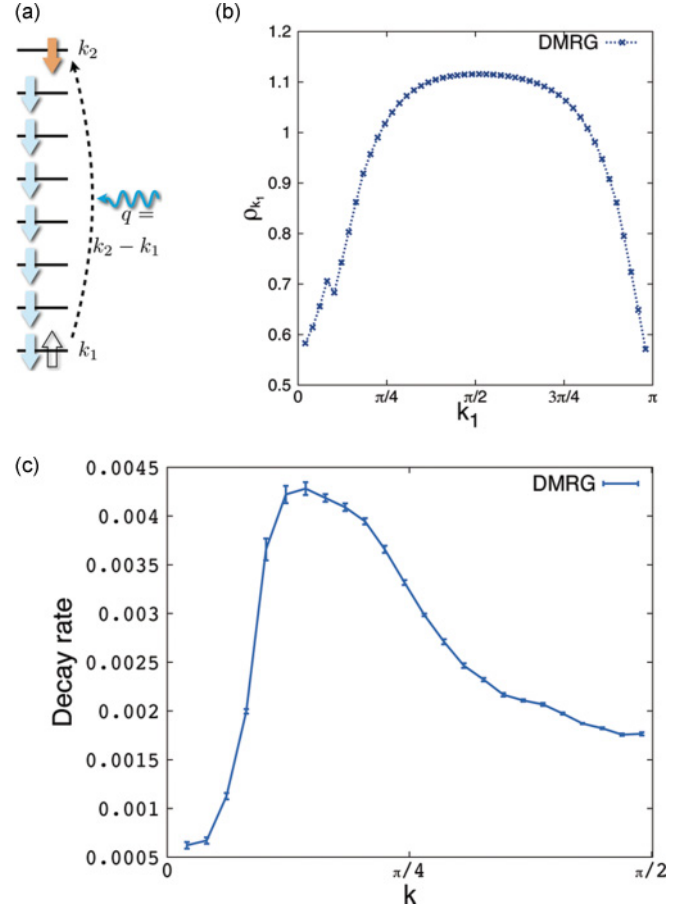


FIG. 7. (Color online) (a) Simplified itinerant electron band structure in k space. Light blue electrons on the left side are electrons initially in the ground state and electrons on the right side are additionally added to the ground state. The process shown correspond to a spin flip of the added electron at $k = k_1$. After the spin flip, the electron has opposite spin with $k = k_2$ and has absorbed a magnon with $q = k_2 - k_1$. (b) Accumulated magnon density ρ_{k_1} as given in Eq. 6, for $L = 48$, $N = 4$, and $J = 0.5$. (c) Decay rates for $L = 48$, $N = 4$, and $J = 0.5$ in dependence of k .

Let us first consider the J dependency. Picking one of the columns and considering only one of the two U values, we immediately recognize that the decay rate shrinks with decreasing J . The exchange strength J determines the time scale on which spins will flip, therefore with decreasing J flipping will be suppressed and the rate decreases. We note that this is different for the decay rate of the spinpolaron, where an increasing J stabilizes each polaron and makes it insensitive to interactions with other electrons. For small J close to or even in the PM phase, the decay rate of the spin-up state increases notably (see $N = 4$). This is natural, since in a paramagnetically ordered system many additional decay channels will open up.

Considering the U dependence we find that with increasing U the rate increases in most cases. In Sec. IV A we have found that an onsite Coulomb interaction has the tendency to order the local spins ferromagnetically. The additional spin-up electron tries to align parallel to the other electrons to minimize interaction energy from the Coulomb potential. This infers a

TABLE B1. Relaxation rates in dependence of the electron number N , J and U . k is set to the lowest possible value $k = \pi/(L + 1)$. The given number of N is the number of electrons taken into account during the ground state calculations, i.e., the spin up electron is in addition to this number. (p) mark parameters, which correspond to the paramagnetic phase.

N	1	2	3	4	6	12
J = 1.0, U = 0			0.002 63 ± 0.000 12	0.001 99 ± 0.000 13	0.001 85 ± 0.000 17	0.000 85 ± 0.000 18
J = 1.0, U = 0.2			0.004 32 ± 0.000 70	0.002 94 ± 0.000 19	0.002 49 ± 0.000 27	0.001 11 ± 0.000 02
J = 0.8, U = 0			0.001 88 ± 0.000 08	0.001 30 ± 0.000 09	0.000 87 ± 0.000 09	0.002 13 ± 0.000 24
J = 0.8, U = 0.2			0.003 03 ± 0.000 21	0.002 21 ± 0.000 17	0.001 84 ± 0.000 17	0.002 38 ± 0.000 38
J = 0.6, U = 0			0.001 15 ± 0.000 05	0.000 78 ± 0.000 05	0.000 81 ± 0.000 07	(p)0.005 08 ± 0.000 31
J = 0.6, U = 0.2			0.002 39 ± 0.000 12	0.001 56 ± 0.000 12		
J = 0.5, U = 0	0.001 04 ± 0.000 02	0.000 97 ± 0.000 03	0.000 82 ± 0.000 03	0.000 62 ± 0.000 04	0.000 66 ± 0.000 05	
J = 0.5, U = 0.2	0.002 33 ± 0.000 04	0.002 22 ± 0.000 01	0.002 05 ± 0.000 08	0.001 26 ± 0.000 11	0.001 41 ± 0.000 13	
J = 0.5, U = 0.4					0.001 42 ± 0.000 21	
J = 0.5, U = 0.6					0.002 45 ± 0.000 18	
J = 0.5, U = 0.8					0.003 84 ± 0.000 45	
J = 0.3, U = 0	0.000 41 ± 0.000 01	0.000 35 ± 0.000 01	0.000 33 ± 0.000 01	(p) 0.001 44 ± 0.000 10	0.001 50 ± 0.000 20	
J = 0.3, U = 0.2	0.001 58 ± 0.000 03	0.001 46 ± 0.000 016	0.001 23 ± 0.000 08	0.000 84 ± 0.000 07		
J = 0.1, U = 0.0	0.000 30 ± 0.000 01		0.000 04 ± 0.000 009	(p) 0.005 93 ± 0.000 24		
J = 0.1, U = 0.2			0.000 61 ± 0.000 03	(p) 0.004 60 ± 0.000 11		

larger decay rate, if U becomes larger. Therefore, this tendency here complies with the influence of the onsite Coulomb interaction found above. Only when a finite U triggers the crossover from the PM to the FM phase, the rate decreases with increasing U (see $N = 4$ and $J = 0.3$). This is obvious since in the PM phase the phase-space arguments presented in Sec. IV D 1 are no longer valid and many more decay channels are possible.

If we increase the number of electrons N in the system and keep the quasimomentum k fixed, we find that the rates decrease with increasing N , for small N deep in the FM phase. This can be explained analog to the discussion in Sec. IV D 1. In the ground state, all initially available electrons fill the spinpolaron-band successively up to $2k_F$ mainly in the spin-down state. An additional spin-up electron can be added to any k mode. In Table II we considered the lowest state $k = \pi/(L + 1)$ in all cases. Considering one of the rows the electron number is increased from left to right and with each electron more in the ground state the respectively next higher k mode is occupied by this additional electron. As a consequence, as shown in Sec. IV D 1, by increasing N we decrease the number of magnons suitable for scattering processes and therefore the decay rate has to decrease. However, in competition to this effect, increasing N means also approaching the PM phase. Then we expect that different and also more decay channels open up, which should lead to an increasing decay rate. This can be seen in Table II for $J = 0.8$ between $N = 6$ and $N = 12$. We have also calculated lifetimes for $N = 7, 9, 10, 11$ (not shown), showing that the decay rates are monotonically increasing with increasing N for large N . For values of N close to half-filling of the conduction band and large values of J , such that we can switch between PM and FM phase, we find decay rates of the order of 0.01. As a consequence, the decay rate depends nonmonotonically on N , it decreases for small values of N deep in the FM phase and increases for larger values of N when the PM phase is approached.

Nonetheless we find the *sweet spot* of the system by *decreasing* the number of electrons going from $N = 4$ to $N = 3$ electrons at $J = 0.1$. There we find that the decay rate of the spin-up electron decreases by two orders of magnitude

when comparing the rates in the PM and FM phase. Still it is important to note that a minimum number of electrons in the system is important to maintain the FM order, especially at finite temperatures.

V. DISCUSSION

In this work we discussed the phase diagram and the spin relaxation properties of the 1D spin-1/2 KLM with Coulomb interaction. We found that a finite onsite or nearest-neighbor interaction favors a FM order of the local spin lattice for small-enough electronic densities. This gives further strong support to the analysis of Refs. 2 and 23, where similar results have been found in 2D semiconductor systems and ^{13}C carbon nanotubes. It provides a pathway to achieve a spontaneous and full polarization of the nuclear spins by lowering the temperature below the critical one. This configuration is desirable for applications in quantum information processing, since it reduces the spin relaxation and decoherence rates of the electronic spins. It is important to notice that a finite crossover temperature can only be expected if the density of electrons is finite. Thus, many electrons are necessary to achieve the FM state. Once the FM state is achieved, one can in principle perform quantum information processing by realizing quantum dots with external gates on time scales which are small compared to the time the nuclear spins need to return to the PM phase. If this is possible one can effectively realize a system consisting of one single electron $N = 1$ in contact with a ferromagnetically ordered nuclear spin lattice. In this case the spin-up state and the spinpolaron are exact eigenstates; that is, the ideal situation with $\Gamma_{\pm} = 0$ is achieved. In this paper we discussed the spin relaxation properties for $N > 1$; that is, we analyzed the question whether the spins in a many-body system could possibly be used as candidates for spin qubits. In Ref. 16 we already found that spinpolarons are indeed very long-living states, indicating that the spinpolaron-spinpolaron interaction is rather weak. However, in this paper we found that the spin-up state is strongly influenced by exchange interaction between the spin-up and spinpolaron states. This exchange process does not require any finite energy and, therefore, cannot even be suppressed by application of a

finite magnetic field. We analyzed in detail the dependence of Γ_+ on the Coulomb interaction U , the exchange interaction J , the particle number N and the quasimomentum k . In the FM phase we found that the rate decreases for smaller values of U , J , k , and larger values for N , unless we approach the PM phase. For appropriate parameter sets we have shown that the lifetime of spin-up states can be two orders of magnitude larger in the FM phase than in the PM phase. However, compared to the lifetime of spin-down spinpolaron states, their lifetime

is orders of magnitudes smaller, regardless of the chosen parameter regime in the FM phase.

ACKNOWLEDGMENTS

We thank D. Loss for valuable discussions. H. Schoeller, U. Schollwöck, and S. Smerat acknowledge the support from the DFG-Forschergruppe 912 on “Coherence and Relaxation Properties of Electron Spins.”

*Sebastian.Smerat@physik.uni-muenchen.de

¹H. O. H. Churchill, A. J. Bestwick, J. W. Harlow, F. Kuemmeth, D. Marcos, C. H. Stwertka, S. K. Watson, and C. M. Marcus, *Nat. Phys.* **5**, 321 (2007).

²B. Braunecker, P. Simon, and D. Loss, *Phys. Rev. Lett.* **102**, 116403 (2009).

³F. Reininghaus, T. Korb, and H. Schoeller, *Phys. Rev. Lett.* **97**, 026803 (2006).

⁴V. Rodrigues, J. Bettini, P. C. Silva, and D. Ugarte, *Phys. Rev. Lett.* **91**, 096801 (2003).

⁵I. V. Krive, R. I. Shekhter, and M. Jonson, *Low Temp. Phys.* **32**, 887 (2006).

⁶H. Tsunetsugu, M. Sigrist, and K. Ueda, *Rev. Mod. Phys.* **69**, 809 (1997).

⁷J. R. Schrieffer and P. A. Wolff, *Phys. Rev. B* **149**, 491 (1966).

⁸M. A. Ruderman and C. Kittel, *Phys. Rev.* **96**, 99 (1954); T. Kasuya, *Prog. Theor. Phys.* **16**, 45 (1956); K. Yosida, *Phys. Rev.* **106**, 893 (1957).

⁹H. Tsunetsugu, M. Sigrist, and K. Ueda, *Phys. Rev. B* **47**, 8345 (1993).

¹⁰G. Honner and M. Gulacsi, *Phys. Rev. Lett.* **78**, 2180 (1997).

¹¹I. P. McCulloch, A. Juozapavicius, A. Rosengren, and M. Gulacsi, *Philos. Mag. Lett.* **81**, 869 (2001).

¹²I. P. McCulloch, A. Juozapavicius, A. Rosengren, and M. Gulacsi, *Phys. Rev. B* **65**, 052410 (2002).

¹³M. Sigrist, H. Tsunetsugu, and K. Ueda, *Phys. Rev. Lett.* **67**, 2211 (1991).

¹⁴P. Richmond, *J. Phys. C: Solid St. Phys.* **3**, 2402 (1970).

¹⁵B. S. Shastry and D. C. Mattis, *Phys. Rev. B* **24**, 5340 (1981).

¹⁶S. Smerat, U. Schollwöck, I. P. McCulloch, and H. Schoeller, *Phys. Rev. B* **79**, 235107 (2009).

¹⁷S. Trebst, H. Monien, A. Grzesik, and M. Sigrist, *Phys. Rev. B* **73**, 165101 (2006).

¹⁸J. Fischer and D. Loss, *Science* **324**, 1277 (2009).

¹⁹D. Loss and D. P. DiVincenzo, *Phys. Rev. A* **57**, 120 (1998).

²⁰R. Hanson, L. P. Kouwenhoven, J. R. Petta, S. Tarucha, and L. M. K. Vandersypen, *Rev. Mod. Phys.* **79**, 1455 (2007).

²¹W. A. Coish and D. Loss, *Phys. Rev. B* **70**, 195340 (2004).

²²W. A. Coish, J. Fischer, and D. Loss, *Phys. Rev. B* **77**, 125329 (2008).

²³P. Simon and D. Loss, *Phys. Rev. Lett.* **98**, 156401 (2007).

²⁴N. D. Mermin and H. Wagner, *Phys. Rev. Lett.* **17**, 1133 (1966).

²⁵P. Bruno, *Phys. Rev. Lett.* **87**, 137203 (2001).

²⁶N. Shibata, T. Nishino, K. Ueda, and C. Ishii, *Phys. Rev. B* **53**, R8828 (1996).

²⁷M. Gulacsi, A. Bussmann-Holder, and A. R. Bishop, *Phys. Rev. B* **71**, 214415 (2005).

²⁸S. R. White, *Phys. Rev. Lett.* **69**, 2863 (1992).

²⁹S. R. White, *Phys. Rev. B* **48**, 10345 (1993).

³⁰U. Schollwöck, *Rev. Mod. Phys.* **77**, 259 (2005).

³¹U. Schollwöck, *Ann. Phys.* **326**, 96 (2010).

³²I. P. McCulloch, *J. Stat. Mech.: Theory Exp.* (2007) P10014.

³³T. D. Kühner and S. R. White, *Phys. Rev. B* **60**, 335 (1999).

³⁴E. Jeckelmann, *Phys. Rev. B* **66**, 045114 (2002).

³⁵Z. Soos and S. Ramasesha, *J. Chem. Phys.* **90**, 1067 (1989).

³⁶S. Ramasesha, S. Pati, and H. Krishnamurthy, *Synth. Met.* **85**, 1019 (1997).